World Scientific
www.worldscientific.com

NON-NEWTONIAN BEHAVIOR IN WEAK FIELD GENERAL RELATIVITY FOR EXTENDED ROTATING SOURCES

H. BALASIN

Institut für Theoretische Physik, Technische Universität Wien,
Wiedner Hauptstr. 8-10/136, A-1040 Vienna, Austria
hbalasin@tph.tuwien.ac.at

D. GRUMILLER

Massachusetts Institute of Technology,
77 Massachusetss Ave, Cambridge, MA 02139, USA
grumil@lns.mit.edu

Exact stationary axially symmetric solutions to the four-dimensional Einstein equations with corotating pressureless perfect fluid sources are studied. A particular solution with an approximately flat rotation curve is discussed in some detail. We find that simple Newtonian arguments overestimate the amount of matter needed to explain such curves by more than 30%. The crucial insight gained by this model is that the Newtonian approximation breaks down in an extended rotating region, even though it is valid locally everywhere. No conflict with solar system tests arises.

Keywords: Dark matter; galactic rotation curves; axially-symmetric stationary perfect fluid solutions in general relativity.

1. Introduction

The problem of the internal dynamics of galaxies is a very old one. It is of special interest because observed non-Keplerian (henceforth "flat") rotation curves[1,2] apparently contradict the simple Newtonian results. These observational facts are usually interpreted in favor of changing the matter model, i.e. introducing dark matter that accounts for the difference between prediction and "experiment"; see e.g. Ref. 3. However, one might also shift the burden to the gravitational theory itself. The most radical change in this line of arguments would result in avoiding dark matter altogether, such as in modified Newtonian dynamics.[4] So far these alternatives are typically at least as unsatisfactory as the dark matter hypothesis itself; see e.g. Refs. 5 and 6.

Taking a closer look at the usual approach, it is Newtonian gravity rather than general relativity (GR) that is applied to the situation of gravitational dynamics

of galaxies. Because the velocity of the stars within a galaxy is small compared to the speed of light and since the gravitational field is very weak (at least a couple of Schwarzschild radii away from a central galactic black hole),[7] the Newtonian approximation seems to be sufficient. However, one has to be careful with such arguments. For instance, it is clear that corrections from GR are smaller in regions where gravity is weaker — and yet the GR distortion of the elliptic orbit of Mercury is visually most pronounced in the aphelion, and not in the perihelion, although gravity is weaker in the former. It is the main purpose of this paper to show that indeed the Newtonian approximation breaks down, even though it might be valid locally everywhere in the galaxy.

The idea of using GR rather than the Newtonian approximation to describe the internal dynamics of galaxies appears to go back to a relatively recent paper by Cooperstock and Tieu.[8] Several errors were pointed out in subsequent publications; see Refs. 9 and 10 and App. B. So it is fair to say that Ref. 8 caused a lot of confusion, interest and critical comments.[9–22] Actually, the approach of taking the nonlinear character of GR more seriously fits in quite well with similar considerations on a cosmological scale.[23–26]

Having a simple framework for the construction of exact solutions at our disposal helps to clarify these important issues. The prime goal of this paper is to provide and discuss such a framework and to point out where and why the Newtonian approximation breaks down.

2. Derivation and Solution of Field Equations

2.1. *Physical assumptions*

We do not discriminate between elliptic, spiral and irregular galaxies, but it is clear that some galaxies will obey the subsequent physical idealizations better than others.

Order-of-magnitude estimates reveal that there are no relevant forces besides gravity in the description of intragalactic dynamics at the percent level. The matter content of a galaxy can be modeled very well by a pressureless perfect fluid. The approximation of vanishing pressure is applicable in the whole galaxy, aside from the very center, where a galactic black hole may be located, and a region close to the rotation axis, where jets might be emitted. Additionally, stationarity and axial symmetry will be imposed, which is reasonable for many galaxies. This implies the existence of two Killing vectors and considerably simplifies the geometry.

We are thus interested in axially symmetric stationary solutions to the Einstein equations ($\kappa = 8\pi$, $G_N = c = 1$)

$$R^{ab} - \frac{1}{2}g^{ab}R = \kappa T^{ab}\,, \tag{1}$$

with the energy–momentum tensor

$$T^{ab} = \rho u^a u^b\,, \tag{2}$$

where ρ, u^a are mass density and 4-velocity, respectively.

2.2. *Deriving the equations*

Theorem 7.1.1 of Ref. 27 (the premises of which apply to the case under consideration) guarantees that, without loss of generality, the line element can be brought into the following form:

$$ds^2 = -K(dt - Nd\phi)^2 + K^{-1}r^2d\phi^2 + \Omega^2(dr^2 + Ldz^2). \tag{3}$$

All of the functions K, N, Ω, L depend solely on the non-Killing coordinates r, z. The coordinate ϕ is 2π-periodic. It should be noted that $K = -\xi^a\xi_a$ is determined by the Killing norm of the timelike Killing vector $\xi^a = \partial_t^a$. We are not interested in inside solutions of black holes here, whence ξ^a is timelike globally.

We shall assume the perfect fluid velocity to be corotating, i.e. $u^a = (u^0(r, z), 0, 0, 0)$. So actually u^a is proportional to the Killing vector $\xi^a = \partial_t^a$. The conservation equation $\nabla_a T^{ab} = 0$ decomposes into

$$\rho u^a \nabla_a u^b = 0, \quad \nabla_a(\rho u^a) = 0. \tag{4}$$

If we suppose that $\rho \neq 0$, then the first equation implies geodesicity of the 4-velocity while the second one expresses stationarity of the mass distribution. This seemingly mild assumption means that the Killing vector ξ^a has to be affine-geodetic and hence K is constant. This is a crucial difference from the matterless case, where no such restriction arises. Without loss of generality one may set $K = 1$ by a rescaling of the time coordinate in regions where $\rho \neq 0$. Henceforth the vacuum case will always be considered as the limit of small ρ. Therefore, $K = 1$ is valid globally.[a] We emphasize that the presence of corotating pressureless perfect fluid sources *simplifies* the dynamics as compared to the vacuum case.

In addition, one may set $L = 1$. The proof as given for example in Ref. 27 is valid only for the vacuum case, but one can show easily that the crucial condition $R^t{}_t + R^\phi{}_\phi = 0$ holds still for a pressureless perfect fluid (albeit it ceases to hold once isotropic pressure is switched on or a cosmological constant is added). Therefore, the line element (3) reduces to

$$ds^2 = -(dt - Nd\phi)^2 + r^2d\phi^2 + e^\nu(dr^2 + dz^2), \tag{5}$$

with the redefinition $\Omega^2 = e^\nu$. From now on we shall exclusively refer to this adapted coordinate system.

Inserting into the Einstein equations (1), (2) establishes (see App. A and also Refs. 28–30)

$$r\nu_z + N_r N_z = 0, \tag{6}$$

$$2r\nu_r + N_r^2 - N_z^2 = 0, \tag{7}$$

---

[a]While this eliminates pure vacuum solutions of technical interest, it retains the physically important solutions where "vacuum" is just an approximation to "very low energy density."

$$\nu_{rr} + \nu_{zz} + \frac{1}{2r^2}\left(N_r^2 + N_z^2\right) = 0, \tag{8}$$

$$N_{rr} - \frac{1}{r}N_r + N_{zz} = 0, \tag{9}$$

$$\frac{1}{r^2}\left(N_r^2 + N_z^2\right) = \kappa\rho e^\nu. \tag{10}$$

Remarkably, the only difference from the perturbative results in Ref. 8 is the factor e^ν on the right-hand side of the last equation.

Before solving these equations we would like to point out that the 3-velocity as seen by an asymptotic observer who is at rest with respect to the center of the galaxy is

$$V(r, z) = \frac{N(r, z)}{r}, \tag{11}$$

provided that $r > N(r, z)$. This may be derived by a standard ADM split of the line element

$$ds^2 = -r^2/(r^2 - N^2)dt^2 + (r^2 - N^2)[d\phi + N/(r^2 - N^2)dt]^2 + e^\nu(dr^2 + dz^2). \tag{12}$$

The standard decomposition of ∂_t^a into lapse and shift yields

$$\partial_t^a = \gamma(n^a + VE_\phi^a), \tag{13}$$

where $n^a = E_t^a$ is the unit normal to the $t = $ const. hypersurfaces and the shift vector is proportional to E_ϕ^a, as expected for angular rotation. The relativistic γ factor is given by $\gamma = 1/\sqrt{1 - V^2}$ with (11). So V is the velocity distribution of the (co)rotating dust as seen by an asymptotic observer who is at rest with respect to the rotation axis. The results above can be found in the classic textbook Ref. 30 (see also Refs. 28 and 29), but we have reviewed them in some detail here in order to make explicit the relevance of each of our assumptions, and also because the result (11) for the velocity is crucial for our discussion.

2.3. Solving the equations

The strategy for solving this coupled system of partial differential equations (PDEs) is as follows. First, we find the general solution to the linear second order PDE (9) for N in terms of a spectral density. Then we use this solution to determine ν from (6)–(8) up to an integration constant. Finally, we solve the last equation (10) for ρ with N and ν as input. To match with input from observations we must fix the spectral density (and thus the function N) accordingly. From (11) we see that N is simply the velocity V times the coordinate r. Thus, the strategy is to take V as an input and to deduce the mass density ρ, rather than the other way around.

2.3.1. *Separation ansatz and zero mode*

We implement now this strategy and focus in this section on (9). The separation ansatz $N = \mathcal{R}(r)\mathcal{Z}(z)$ yields $\mathcal{Z}_{zz} = k\mathcal{Z}$, with the separation constant $k \in \mathbb{R}$. Because of reflection symmetry, $N(r,z) = N(r,-z)$. Therefore, $\mathcal{Z}(z) = \int dk A(k)\mathcal{Z}(k,z)$ is solely composed of even modes, $\mathcal{Z}(k,z) = \cosh\left(\sqrt{k}z\right)$. If $k > 0$, then these modes diverge exponentially for $|z| \to \infty$. This is unphysical behavior. In Ref. 8 a positive value for k *and* falloff behavior at infinity was achieved by employing the nonsmooth modes $\mathcal{Z}(k,z) = e^{-\sqrt{k}|z|}$, which satisfy (9) for $|z| > 0$ only. Consequently, there are sources localized at $z = 0$. We show in App. B that either the weak energy condition is violated in the whole galactic plane or the pressure must be negative; so these sources are unphysical and contradict our assumption that of vanishing pressure. Thus, we have no choice but to assume that $k = -\lambda^2$, with $\lambda \in \mathbb{R}_0^+$ yielding the modes $\mathcal{Z}(\lambda,z) = \cos(\lambda z)$.

Let us address first the zero mode, $\lambda = 0$. Without loss of generality $\mathcal{Z} = 1$ and $\mathcal{R} = A_0 + B_0 r^2$. Thus, the zero mode solution reads

$$N_0 = A_0 + B_0 r^2. \tag{14}$$

We consider first the simplest case, $B_0 = 0$. Then the velocity (11) is given by A_0/r and exceeds the speed of light for small r. While this is unpleasant, we note that the Einstein equations (6)–(10) are invariant under the constant shift $N \to N - A_0$. So the constant A_0 may be absorbed into a redefinition of the time variable. Thus, in addition to the falloff condition for $|z| \to \infty$ exploited above and to the falloff condition for $r \to \infty$ exploited below, we have to impose a condition to fix A_0, for example by requiring that $N(0,0) = 0$. This will be discussed in more detail below; right now we simply fix $A_0 = 0$. Then, if $B_0 \neq 0$, the velocity profile $V = B_0 r$ is linear, as expected from Newtonian gravity for a disk rotating with constant angular velocity. To get a first glimpse of possible differences between Newton and Einstein, we consider the simplest case where only the zero mode is switched on, i.e. $V \propto r$, and restrict ourselves to the galactic plane $z = 0$. In Newtonian gravity one obtains

$$\rho_N(r) = \text{const.} \tag{15}$$

However, general relativity behaves differently: plugging $N \propto r^2$, into (7) yields $\nu \propto r^2$, with a negative proportionality constant. The unperturbed Einstein equation (10) establishes ($\alpha \in \mathbb{R}$)

$$\rho(r) \propto e^{\alpha^2 r^2}. \tag{16}$$

Conceptually (although not physically) this is an important result: given as input the same velocity profile in the galactic plane, $V \propto r$, Newtonian and general-relativistic calculations yield different results for the mass density, even though locally the quantity ρ as given in (16) can always be matched to the Newtonian ρ_N in (15) by adjusting appropriately in ν the integration constant α. Thus, only for a small region of space–time is the Newtonian picture correct. However, the zero

mode obviously is unphysical, because for large values of r the velocity V would exceed the speed of light. Thus, from now on we set $B_0 = 0$, i.e. the zero mode is dropped.

2.3.2. *Generic modes*

In order to get the generic modes we use the rescaled variable $x = \lambda r$ and obtain from the separation ansatz above the ordinary differential equation

$$\mathcal{R}'' - \frac{1}{x}\mathcal{R}' - \mathcal{R} = 0 \,, \tag{17}$$

where the prime denotes differentiation with respect to x. It can be solved by standard methods. The result for $N = \mathcal{R}\mathcal{Z}$ is given by

$$N(r,z) = \int_0^\infty d\lambda \cos(\lambda z)(r\lambda)\left[A(\lambda)K_1(\lambda r) + B(\lambda)I_1(\lambda r)\right]. \tag{18}$$

The spectral densities $A(\lambda)$ and $B(\lambda)$ may be chosen according to the behavior required of $N(r,z)$. The functions I_1 and K_1 are modified Bessel functions of the first and the second kind, respectively (the latter is also known as the Macdonald function). We note that I_1 blows up exponentially for large values of r, which is unphysical. Therefore, we set $B(\lambda) = 0$. The function K_1 falls off exponentially for large values of r and diverges like $1/r$ near $r = 0$. However, this divergence is compensated for by a linear prefactor, so the integrand is well defined for any sufficiently regular $A(\lambda)$. We plot $x \cdot K_1(x)$ in Fig. 1. The technical observation

$$\int_0^\infty dx x K_1(x) \cos\left(\frac{ax}{r}\right) = \frac{\pi}{2}\frac{r^3}{(a^2 + r^2)^{3/2}} \tag{19}$$
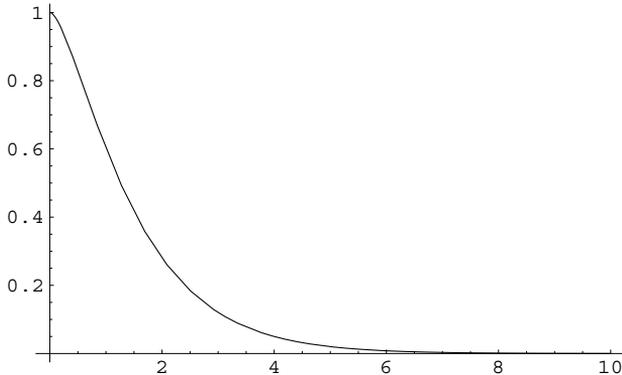
will be very useful below.

Fig. 1. $x \cdot K_1(x)$.

To summarize, the general solution of (9) is consistent with physical falloff behavior $|z|, r \to \infty$, and with the absence of spurious sources in the galactic plane $z = 0$, is given by

$$N(r, z) = A_0 + \int_0^\infty d\lambda \cos(\lambda z)(r\lambda)A(\lambda)K_1(\lambda r). \tag{20}$$

The constant A_0 has to be fixed by some additional boundary condition, for example by requiring a certain behavior of N as $r \to 0$. This can be done efficiently by first setting $A_0 = 0$, then designing a useful spectral density $A(\lambda)$, and finally shifting N by a suitable constant.

2.4. *Fixing the spectral density*

The choice of $A(\lambda)$ determines not only the radial velocity profile, but also the z dependence of N. Thus, the behavior in the z direction is determined uniquely by the behavior in the r direction, and vice versa. This is good for the predictability of the model, because one may fit one kind of behavior and predict the other, in addition to predicting the matter density. Instead of fixing $A(\lambda)$ directly we found it useful to perform first a Fourier transformation,

$$A(\lambda) = \frac{2}{\pi} \int_0^\infty dx\, C(x) \cos(\lambda x), \tag{21}$$

where $A(\lambda)$ is determined in terms of a (Fourier-)transformed spectral density $C(x)$. This allows us to represent $V(r, 0)$ as

$$V(r, 0) = r \int_0^\infty dx \frac{C(x)}{(x^2 + r^2)^{3/2}} = \frac{1}{r} \int_0^\infty d\tilde{x} \frac{C(\tilde{x}r)}{(\tilde{x}^2 + 1)^{3/2}}, \tag{22}$$

with some arbitrary function $C(x)$, which we may again call "spectral density." It is evident that for $C \propto x^2$ the velocity profile is linear in r, while for $C \propto x$ the velocity profile is flat. Therefore, this purely technical step is very useful for matching with observational data. The function $N(r > 0, z)$ reads

$$N(r > 0, z) = \frac{r^2}{2} \int_0^\infty dx\, C(x)([(z+x)^2 + r^2]^{-3/2} + [(z-x)^2 + r^2]^{-3/2}). \tag{23a}$$

For $r = 0$ we obtain

$$N(0, z \geq 0) = \frac{2}{\pi} \int_0^\infty d\lambda \cos(\lambda z) \int_0^\infty dx\, C(x) \cos(\lambda x) = C(z), \tag{23b}$$

provided that the function $C(z)$ is sufficiently well behaved. The result for $z < 0$ is obtained from reflection symmetry.

For physical applications one still has to choose the spectral density C suitably. It is instructive to consider the case of constant C: the function $N(r, z)$ turns out to be constant, which is problematic because for arbitrarily small values of r the
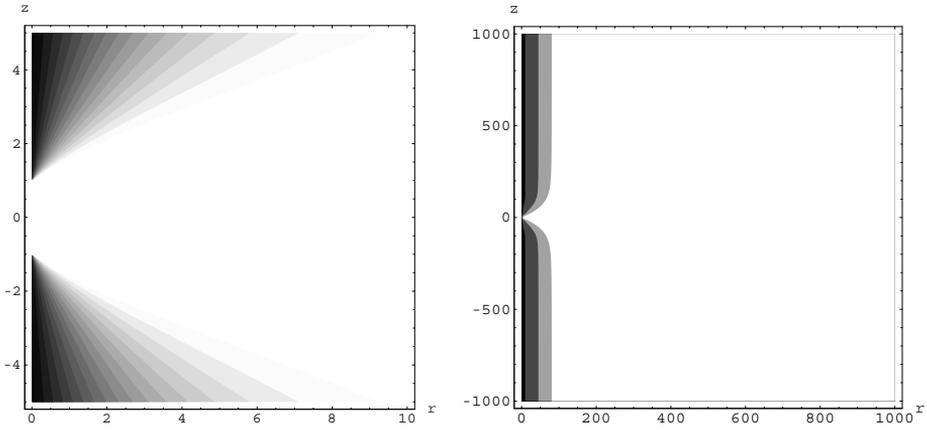
Fig. 2.   Contour plot of $V(r,z)$ [$N(r,z) \gtrsim r$ in the black region].

function $V(r,z)$ as defined in (11) grows without bound. In model building we have seen this feature to be generic, rather than an artifact of a particular choice of C: if the velocity profile is taken from experimental data, it turns out that for some values of z there will always be in a region close to the axis $r = 0$, where V exceeds unity. This is a clear signal of the breakdown of our assumptions. For galaxies emitting jets this is not unexpected, since jets emitted along the axis are not pressureless. Also, the region around eventual central galactic black holes is located on the axis, so perhaps there is good (physical) reason for these regions not being described by a dustlike matter model. It is not the purpose of the current paper to further discuss these regions, where closed timelike curves may arise, similar to the Gödel universe (the appearance of such regions appears to be a generic feature of axially symmetric stationary solutions). Therefore, we cut out the domains where $N(r,z) \gtrsim r$ and blithely ignore them (see Fig. 2). While this is clearly unsatisfactory, it appears to be not much worse than ignoring the problem with cusps in Newtonian cold dark matter models.

3. A Toy Model for Galaxies

3.1. *Input*

Experimental data imply[1,2] that for small values of r the velocity should increase linearly with r and for intermediate values of r it should yield an approximately flat profile. Asymptotically it should fall off like $1/r$ in order to match the Kerr solution.[31] Moreover, it is required that $V(0,z)$ be regular for $|z| < r_0$, where the quantity r_0 is of the order of $1\,\mathrm{kpc} \approx 3 \times 10^{54}$, which allows us to describe also the bulge region of the galaxy within our model.

With these remarks in mind we propose a simple three-parameter function for C (θ is the step function):

$$C(x) = (x - r_0)(\theta(x - r_0) - \theta(x - R)) + (R - r_0)\theta(x - R). \qquad (24)$$

The three parameters, V_0, r_0, R, have to be chosen appropriately. The quantity V_0 is of the order of the velocity in the flat regime ($V_0 \approx 200\,\text{km/s} \approx 7 \times 10^{-4}$). The bulge radius r_0 is set to $1\,\text{kpc}$ and R to $100\,\text{kpc}$. Note that C is smooth besides the points $x = r_0, R$. We stress that a smooth version of C may be chosen to improve the model (also, other refinements may be implemented according to phenomenological necessities), but we want to keep the model simple and exactly soluble for pedagogic reasons.

3.2. *Output*

From (24) and (23a) we obtain

$$N(r,z) = V_0(R - r_0) + \frac{V_0}{2}\sum_{\pm}(\sqrt{(z \pm r_0)^2 + r^2} - \sqrt{(z \pm R)^2 + r^2}). \qquad (25)$$

It may be checked that (25) indeed satisfies (9) up to some distributional contributions at $r = 0, |z| \geq r_0$. The latter lie in the region we are not able to describe. It is an open problem how to deal with that region along the axis (even in the Newtonian approach), and we shall not address this issue here any further. However, as we shall see now, these critical regions lie outside the toy galaxy, i.e. at values $|z| \geq r_0$, and are localized along the z axis. Therefore, we are able to draw meaningful conclusions for galactic rotation curves.

Contour plots of the velocity are depicted in Fig. 2. The darker the region, the higher the velocity. One unit corresponds to $1\,\text{kpc}$ in these plots. The left figure shows that indeed the function $V(0, z)$ is regular until $|z| = 1\,\text{kpc}$, while the right figure reveals that on large scales the region we had to cut out stays close to the axis. The velocity profile in the galactic disk reads

$$V(r,0) = \frac{V_0}{r}\left(R - r_0 + \sqrt{r_0^2 + r^2} - \sqrt{R^2 + r^2}\right). \qquad (26)$$

Various limits are $V(r \ll r_0, 0) \approx r\,V_0/2r_0$, $V(r_0 \ll r \ll R, 0) \approx V_0$ and $V(R \ll r, 0) \approx V_0 R/r$. Figure 3 depicts the ratio $V(r,0)/V_0$ up to $20\,\text{kpc}$. The velocity profile approximately behaves as required. Remarkably, r_0 determines also the transition between the linear and the flat regime of the velocity profile, whereas the choice of R determines the transition between the flat and the asymptotic regime. Thus, within this model the thickness of the bulge may be predicted from the velocity profile.

We have calculated the function ν by solving (6)–(8) and found that it is negligible up to the subpermil level, besides the integration constant. This is mainly due to the fact that $V_0^2/4 \approx 10^{-7} \ll 1$. Thus, for most practical purposes $\nu(r, z) \approx -\ln\beta = \text{const.}$, where β is an integration constant. The density may now be derived from (10),

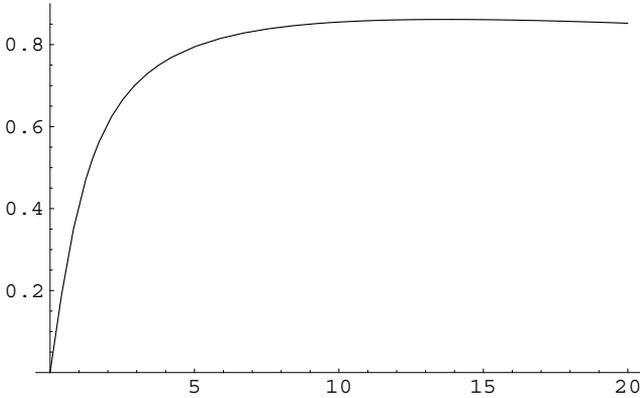$$\kappa\rho(r,z) \approx \frac{\beta}{r^2}\left(N_r^2 + N_z^2\right). \qquad (27)$$

Fig. 3. $V(r,0)/V_0$ plotted up to $20\,\mathrm{kpc}$.

Integrating the density over the white region on the right, Fig. 2 yields about 10^{11} solar masses for the total mass, which is not unreasonable. The density within the galactic disk behaves as follows: for $r \to 0$ it goes to a constant $(\beta V_0^2/r_0^2)$, for $r_0 \ll r \ll R$ it falls off like $1/r^2$ and for $r \gg R$ it falls off like $1/r^6$.

3.3. *Comparison with Newton*

We shall now compare the mass density for a given velocity profile as predicted by simple Newtonian considerations with the GR mass density calculated above. We shall restrict ourselves to the galactic plane for simplicity.

The Newtonian density for a given velocity profile may be derived naively from equating the kinetic energy per mass, $V^2/2$, with the potential energy per mass, $(4\pi \int \rho_N r_s^2 \, dr_s)/r_s$. The quantity r_s denotes the spherical radius $r_s^2 = r^2 + z^2$, which coincides with the axial one in the galactic plane. Differentiation establishes

$$\rho_N(r_s, 0) = \rho_N(r, 0) \propto \frac{V^2 + 2rVV'}{r^2} \; . \tag{28}$$

The proportionality constant is known, but irrelevant as we are interested solely in the ratio ρ/ρ_N and ρ contains still an arbitrary multiplicative constant β which has to be fixed.

In order to get a result which is robust with respect to slight changes in the spectral density C, we assume an *arbitrary* function C with the following two properties: (1) it leads to an approximately linear velocity profile for small r ("small" meaning small compared to $1\,\mathrm{kpc}$, but not so small that one is at the scale of the galactic black hole, e.g. around 1–$100\,\mathrm{pc}$); (2) it leads to an approximately flat velocity profile for large r ("large" meaning large compared to sub-kpc but still smaller than the whole galaxy, e.g. around 1–$20\,\mathrm{kpc}$). For any given velocity profile

$V(r,0)$ we may compare the Newtonian prediction with the one from GR[b]:

$$\frac{\rho}{\rho_N} = \beta \left(1 + \frac{r^2 (V')^2}{V^2 + 2rVV'} \right). \tag{29}$$

Clearly, at each point in the galaxy we may achieve perfect agreement between Newtonian and GR predictions by choosing β appropriately. This reflects the local validity of the Newtonian approximation. However, it is important to realize that globally β can only be chosen once. Because usually one requires consistency between Newtonian and GR predictions in the region where luminous matter dominates, i.e. in the linear regime ($V \propto r$), let us now fix β such that

$$\left. \frac{\rho}{\rho_N} \right|_{\text{linear}} = 1 = \beta \left(1 + \frac{r^2}{3r^2} \right) = \beta \frac{4}{3}. \tag{30}$$

Consequently, in the flat regime ($V = \text{const.}$) we obtain

$$\left. \frac{\rho}{\rho_N} \right|_{\text{flat}} = \beta = \frac{3}{4}. \tag{31}$$

Thus, requiring consistency between Newton and GR in the linear regime necessarily leads to a considerable deviation in the flat regime: Newtonian estimates require 133% of the mass density as compared to GR calculations in order to get the same velocity profile. We reiterate the key observation: the integration constant β emerging in the GR solution can only be fixed once globally.

We stress that these considerations are of relevance only to extended rotating sources. Thus, they play no role in solar system tests because there the main gravitational source is localized in the Sun.

4. Conclusions

Using a simple model for a galaxy we could show that the Newtonian approximation overestimates the amount of matter by about a third, whereas GR reduces the amount of dark matter needed to explain the flat rotation curves. This does not imply that exotic dark matter does not exist, as insinuated by Ref. 8. After all, dark matter is a "500% effect" (meaning that there is about five times as much dark matter in the universe as ordinary matter) and there are several independent measurements and arguments which suggest the existence of dark matter, for example from microlensing.[32] But as astrophysical measurements reach unprecedented accuracy the unexpected GR correction in the 30% range predicted in our paper certainly will not be negligible. It is emphasized that this prediction has essentially been independent of the particular choice of the spectral density C.

It would be interesting to check the robustness of our results by relaxing some of our assumptions — particularly corotation — or (some of) the symmetry requirements.

---

[b]Obviously for the Keplerian profile $V \propto 1/\sqrt{r}$, the ratio (29) becomes singular as a consequence of $\rho_N = 0$.

Acknowledgments

Appendix A. Ricci Tensor

In the adapted coordinate system (5) the components of the Ricci tensor read

$$R_{tt} = \frac{e^{-\nu}}{2r^2}\left(N_r^2 + N_z^2\right), \tag{A.1a}$$

$$R_{t\phi} = \frac{e^{-\nu}}{2r^2}\left(-N(N_r^2 + N_z^2) - r^2\left(N_{rr} - \frac{1}{r}N_r + N_{zz}\right)\right), \tag{A.1b}$$

$$R_{tr} = 0 = R_{tz}, \tag{A.1c}$$

$$R_{\phi\phi} = \frac{e^{-\nu}}{2r^2}\left((r^2 + N^2)(N_r^2 + N_z^2) + 2r^2N\left(N_{rr} - \frac{1}{r}N_r + N_{zz}\right)\right), \tag{A.1d}$$

$$R_{\phi r} = 0 = R_{\phi z}, \tag{A.1e}$$

$$R_{rr} = \frac{1}{2}\left(-\nu_{rr} - \nu_{zz} + \frac{1}{r^2}N_r^2 + \frac{1}{r}\nu_r\right), \tag{A.1f}$$

$$R_{rz} = \frac{1}{2}\left(\frac{1}{r}\nu_z + \frac{1}{r^2}N_r N_z\right), \tag{A.1g}$$

$$R_{zz} = \frac{1}{2}\left(-\nu_{rr} - \nu_{zz} + \frac{1}{r^2}N_z^2 - \frac{1}{r}\nu_r\right). \tag{A.1h}$$

As usual, on the right-hand side the indices r and z denote partial derivatives with respect to the corresponding coordinate, and repeated indices denote repeated partial derivatives, e.g. $N_{rr} := \partial_r \partial_r N(r, z)$.

Appendix B. Localized Exotic Energy–Momentum Tensor

In Ref. 8 the expression (J_1 is a Bessel function of the first kind)

$$N(r,z) = -\sum_n C(k_n)\sqrt{k_n}\, r J_1(\sqrt{k_n}r)e^{-\sqrt{k_n}|z|} \tag{B.1}$$

has been used, which is nonsmooth at $z = 0$. According to the surface-layer formalism of Israel, a localized energy–momentum contribution is generated by the jump in the extrinsic curvature across the surface $z = 0$,

$$T_{ab}^{\mathrm{loc}} = \kappa\delta(z)([K_{ab}] - h_{ab}[K]), \tag{B.2}$$

where h_{ab} denotes the (continuous) induced metric and $[K_{ab}] = K_{ab}^+ - K_{ab}^-$ the jump of the extrinsic curvature. Inserting into the definition ($\mathcal{L}_{n^e}$ denotes the Lie derivative along $n^c = E_z^c = e^{-\nu/2}\partial_z^c$)

$$K_{ab} = \frac{1}{2}\mathcal{L}_{n^c}h_{ab}, \tag{B.3}$$

with $h_{ab} = -(dt - N\,d\phi)_{ab}^2 + r^2 d\phi_{ab}^2 + e^\nu dr_{ab}^2$, we find that

$$K_{ab} = \frac{e^{-\nu/2}}{2}(2(dt - N\,d\phi)N_z\,d\phi + e^\nu \nu_z\,dr^2)_{ab}. \tag{B.4}$$

The discontinuity $[N_z] = 2\sum_n C(k_n)k_n r J_1(\sqrt{k_n}r)$ inserted into (6) implies another discontinuity, $[\nu_z] = -N_r[N_z]/r$. The jump of the extrinsic curvature

$$[K_{ab}] = \frac{e^{-\nu/2}}{2}\left(2[N_z](dt - N\,d\phi)d\phi + e^\nu[\nu_z]dr^2\right)_{ab} \tag{B.5}$$

yields the localized (effectively (1+1)-dimensional) energy–momentum tensor

$$T_{ab}^{\mathrm{loc}} = \kappa\delta(z)\frac{e^{-\nu/2}}{2r}N_r[N_z]\tilde{g}_{ab} := P_I\tilde{g}_{ab}, \tag{B.6}$$

with the (1+1)-dimensional metric

$$\tilde{g}_{ab} = -(dt - N\,d\phi)_{ab}^2 + r^2 d\phi_{ab}^2 + \frac{2r}{N_r}((dt - N\,d\phi)d\phi)_{ab}. \tag{B.7}$$

We note that both the four- and two-dimensional traces yield $\mathrm{Tr}\,T_{ab}^{\mathrm{loc}} = 2P_I$, whereas both the four- and two-dimensional contractions with the timelike Killing vector ξ^a yield the energy density

$$\rho_I := T_{ab}^{\mathrm{loc}}\xi^a\xi^a = -P_I. \tag{B.8}$$

It saturates the strong energy condition, and additionally obeys the weak energy condition if $N_r[N_z] \leq 0$ at $z = 0$ for all r. We may interpret the induced energy–momentum tensor as that of a (1+1)-dimensional perfect fluid with mass density ρ_I and pressure P_I. So either the pressure is negative or the weak energy condition is violated. In any case we have exotic matter.[c] Moreover, clearly, one of our

---

[c]One can decide between these two possibilities by taking a certain velocity profile in the galactic plane, inserting into (11), calculating N_r and checking its sign. For monomials $V = a^2 r^\alpha$ with $\alpha > -1$, one gets $N_r > 0$. In addition, one needs an argument for the sign of $[N_z]$.

basic assumptions that led to the adapted line element (5), namely the absence of pressure, is violated by (B.6).

So the Cooperstock–Tieu model is unphysical and inconsistent, as pointed out in numerous comments. Where applicable, results of this appendix essentially agree with those of Refs. 9 and 10 (We have the factor $\frac{\kappa}{2}e^{-\nu/2}$ in (B.6) instead of $e^{-\nu}$ as in Ref. 8, but this is a minor discrepancy and of no relevance to the argument that matter in the galactic plane is exotic in the Cooperstock–Tieu model).

References

1. V. C. Rubin, N. Thonnard and W. K. Ford, Jr., *Astrophys. J.* **238** (1980) 471.
2. A. Bosma *Astron. J.* **86** (1981) 1791.
3. M. Persic, P. Salucci and F. Stel, *Mon. Not. R. Astron. Soc.* **281** (1996) 27 [astro-ph/9506004].
4. M. Milgrom, *Astrophys. J.* **270** (1983) 365.
5. V. V. Zhytnikov and J. M. Nester, *Phys. Rev. Lett.* **73** (1994) 2950 [gr-qc/9410002].
6. A. Aguirre, C. P. Burgess, A. Friedland and D. Nolte, *Class. Quant. Grav.* **18** (2001) R223 [hep-ph/0105083].
7. A. Eckart and R. Genzel, *Nature* **383** (1996) 417.
8. F. I. Cooperstock and S. Tieu, astro-ph/0507619.
9. M. Korzynski, astro-ph/0508377.
10. D. Vogt and P. S. Letelier, astro-ph/0510750.
11. D. Garfinkle, gr-qc/0511082.
12. F. I. Cooperstock and S. Tieu, astro-ph/0512048.
13. D. Vogt and P. S. Letelier, astro-ph/0512553.
14. D. J. Cross, astro-ph/0601191.
15. M. Rocek and P. van Nieuwenhuizen, gr-qc/0603010.
16. L. Bratek, J. Jalocha and M. Kutschera, astro-ph/0603791.
17. B. Fuchs and S. Phleps, *New Astron.* **11** (2006) 608 [astro-ph/0604022].
18. V. Kostov, astro-ph/0604395.
19. D. Alba and L. Lusanna, gr-qc/0604086.
20. L. Lusanna, gr-qc/0604120.
21. M. D. Maia, A. J. S. Capistrano and D. Muller, astro-ph/0605688.
22. T. Zingg, A. Aste and D. Trautmann, astro-ph/0608299.
23. A. Hosoya, T. Buchert and M. Morita, *Phys. Rev. Lett* **92** (2004) 141302 [gr-qc/0402076].
24. G. F. R. Ellis and T. Buchert, *Phys. Lett. A* **347** (2005) 38–46 [gr-qc/0506106].
25. A. A. Coley, N. Pelavas and R. M. Zalaletdinov, *Phys. Rev. Lett.* **95** (2005) 151102 [gr-qc/0504115].
26. D. L. Wiltshire, gr-qc/0702082.
27. R. M. Wald, *General Relativity* (The University of Chicago Press, 1984).
28. W. J. van Stockum, *Proc. Roy. Soc. Edinburgh* **57** (1937) 135.
29. W. Bonnor, *J. Phys. A* **10** (1977) 1673.
30. H. Stephani, D. Kramer, M. MacCallum, C. Hoenselaers and E. Herlt, *Exact Solutions of Einstein's Field Equations* (Cambridge University Press, 2003).
31. R. P. Kerr, *Phys. Rev. Lett.* **11** (1963) 237.
32. MACHO Collab. (C. Alcock *et al.*), *Phys. Rev. Lett.* **74** (1995) 2867 [astro-ph/9501091].